Contents lists available at ScienceDirect

Arabian Journal of Chemistry

journal homepage: www.ksu.edu.sa

Original article

A novel trifluoromethyl quinoline derivative targeting SGK1 inducing autophagy and apoptosis via regulating mTOR/FOXO3a pathway in glioblastoma

Yu-feng Xiong [a,1], Cheng Li [b,c,1], Jia Yu [b,c], Xiaozhong Chen [e], Sha Cheng [b,c], Xin-yu Liu [b,c], Bi-xue Xu [b,c], Xiao Hu [a,d,*], Guang-can Xu [b,c,**], Heng Luo [b,c,**]

[a] GuiZhou University Medical College, Guiyang 550025, Guizhou Province, China
[b] State Key Laboratory of Functions and Applications of Medicinal Plants, Guizhou Medical University, Guiyang 550014, China
[c] Natural Products Research Center of Guizhou Province, Guiyang 550014, China
[d] Department of Neurology, Guizhou Provincial People's Hospital, Guiyang 550002, China
[e] Department of Neurosurgery, Affiliated Hospital of Zunyi Medical University, Zunyi 563000, Guizhou Province, China

ARTICLE INFO

Keywords:
Quinoline Derivative
Glioblastoma multiforme
Autophagy
SGK1
FOXO3a/mTOR signaling pathway

ABSTRACT

Glioblastoma (GBM) is known for its aggressive nature and poor prognosis, with currently no effective treatment available. Research has shown that introducing fluorinated functional groups into different parts of natural product quinoline significantly affects its anti-tumor activity. Therefore, this study synthesized the trifluoromethyl quinoline derivative **FKL296** to investigate its anti-tumor effect on GBM and reveal its mechanism of action. *In vitro* and *in vivo* studies have shown that **FKL296** effectively inhibitd the growth of GBM and is relatively safe and low toxicity, whice also induced cell apoptosis and autophagy. Additionally, protein kinase profiling and molecular docking analyses have revealed a strong binding affinity between **FKL296** and SGK1. Cellular thermal shift assay experiments have confirmed the targeting of SGK1 by **FKL296** and its role in enhancing SGK1 stability. Bioinformatics analysis and pathway validation indicated that **FKL296** targeted SGK1 and inhibited autophagy in tumor cells through the mTOR/FOXO3a signaling pathway. In summary, **FKL296** may become a promising drug for the treatment of GBM.

1. Introduction

Glioblastoma multiforme (GBM), according to the classification of the World Health Organization (WHO), classified as high-grade type IV glioma. It is highly invasive and has an extremely poor prognosis, with an average five-year survival rate of 7.2 % and an average length of survival 15 months (Onishi et al., 2022, GBD, 2019). Currently, GBM treatment consists of multimodal therapy, involving surgery, chemotherapy, and radiation with temozolomide (TMZ) serving as the major chemotherapeutic drug (Erices et al., 2023, Tan et al., 2020). Despite multimodal therapy has improved the short-term survival rate of GBM patients, the overall prognosis for patients remains poor, particularly the five-year survival rate (Wan et al., 2023). It has been demonstrated that long-term treatment with TMZ, which leads to the methylation of O6-methylguanine-DNA methyltransferase (MGMT), the mutation of isocitrate dehydrogenase (IDH), and a multitude of abnormal signaling cascades, results in significant drug resistance (Butler M et al., 2020). TMZ, known as a cytotoxic monofunctional alkylating agent, elicits serious side effects within the body (Liu et al., 2019). Therefore, finding new and safe drugs for treating glioblastoma has become a top priority.

Autophagy is a lysosomal dependent degradation process, and unrestricted autophagy may lead to cell death by selectively degrading molecules or organelles that promote survival (Klionsky et al., 2000, Dikic et al., 2018, Liu et al., 2023). Studies have shown that autophagy

* Corresponding author at: Department of Neurology, Guizhou Provincial People's Hospital, Guiyang 550002, China.
** Corresponding authors at: State Key Laboratory of Functions and Applications of Medicinal Plants, Guizhou Medical University, Guiyang 550014, China.
E-mail addresses: gjwin520@163.com, 2370774483@qq.com (Y.-f. Xiong), licheng1999@qq.com (C. Li), yu_jia@gmc.edu.cn (J. Yu), chengsha@gzcnp.cn (S. Cheng), 1073392923@qq.com (X.-y. Liu), bixue_xu@126.com (B.-x. Xu), huxiao@gz5055.com, hu_xiao119@163.com (X. Hu), xgc0707@163.com (G.-c. Xu), luo_heng@gmc.edu.cn, luoheng71050@aliyun.com (H. Luo).
[1] These authors contributed equally to this work.

https://doi.org/10.1016/j.arabjc.2024.105909
Received 30 April 2024; Accepted 14 July 2024
Available online 16 July 2024

can regulate the development of glioblastoma. Zheng Jinxiang et al. found that sino-wcj-33 (SW33), a derivative of sinomenine, blocks the cell cycle in the G2/M phase, induces mitochondrial dependent apoptosis, and induces autophagy through the PI3K/AKT/mTOR and AMPK/mTOR pathways (Zheng et al., 2021). Li Huicheng et al. found that in A172 and U-373MG cells treated with luteolin, cell viability decreased in a concentration and time-dependent manner, and autophagy was induced (Lee et al., 2021). Therefore, a deeper understanding of the regulatory mechanisms of autophagy provides new targets and therapeutic directions for tumor treatment.

In cancer therapy, natural products and their derivatives are rich sources for the discovery of novel small-molecule compounds with anticancer properties. Nitrogen-containing heterocycles play an important role in the development of drugs for cancer treatment (Li et al., 2017, Freitas et al., 2014). Quinoline and its derivatives are nitrogen-containing heterocyclic compounds with a wide range of pharmacological activities (Jain et al., 2016). Quinoline scaffolds have been used to develop antibacterial (Blaskovich et al., 2019) and anticancer (Kannaiyan et al., 2019) drugs. Our previous research has shown that fluoroquinoline derivatives can effectively target HDAC1, leading to increased histone acetylation in cervical cancer cellst (Zhang et al., 2024), this indicates that introducing fluorinated functional groups into different parts of the natural product quinoline significantly affects its anti-tumor activity. Therefore, we screened **FKL** derivatives and found that **FKL296** has good activity against GBM cells. However, the molecular mechanism of **FKL** derivatives in glioblastoma is still unknown.

In this study, to explore the autophagy effect of **FKL296**, which targets SGK1 on glioblastoma activation via the mTOR/FOXO3a signaling pathway, we investigated the anti-GBM effects of **FKL296** *in vivo* and *in vitro*. We have demonstrated that **FKL296** inhibits the proliferation, migration, and invasion of glioblastoma cells, while also triggering apoptosis and autophagy in GBM cells. In addition, **FKL296** exhibits thermal stability toward SGK1 and induces autophagy in GBM cells by activating the FOXO3a/mTOR pathway. Furthermore, the results showed that overexpression of SGK1 inhibits autophagy in GBM cells, which can be reserved with **FKL296**. As a result, this study demonstrates that targeting SGK1 with **FKL296** induces autophagy in GBM via the FOXO3a/mTOR signaling pathway, providing novel insights and strategies for utilizing **FKL296** in GBM therapy.

2. Materials and methods

2.1. Chemicals, Reagents, and instruments

FKL296 was synthesized by the Guizhou Provincial Natural Products Research Center (purity > 98 %). **FKL296** was dissolved in dimethyl sulfoxide (DMSO), and prepared into 2×10^4 μM stock solution. The specific inhibitor of the SGK1 kinase activity SI113 was purchased from TargetMOL (T9589). Temozolomide (TMZ) was purchased from Medchemexpress. TMZ was dissolved in dimethyl sulfoxide (DMSO) to prepare a 50 mM stock solution. Dulbecco Modified Eagle Medium (DMEM) was purchased from Gibco (Waltham, MA, USA). Trypsin was purchased from Bioindustry (Kibbutzbet-Hymek, Israel). DMSO was purchased from Zhiyuan Chemical Reagents Co., Ltd (Tianjin, China). Transwell inserts were purchased from Corning (New York, USA). The BCA protein assay kit was purchased from Bi (Shanghai, China). The microplate reader was purchased from BioTek (Winooski, VE, USA). CO_2 cell cultures were purchased from Thermo Fisher Scientific (Waltham, MA, USA). Allegra X-15R high-speed centrifuge was purchased from Beckman (Brea, CA, USA). ACEA NovoCyte Flow cytometer was purchased from BD Biosciences (USA) Leica inverted fluorescence microscope was purchased from Leica (Weizlaal, Germany).

2.2. Antibodies

SGK1 antibody (Cat#R381169, 1:1000 dilution), FOXO3a antibody (Cat#R26154, 1:1000 dilution), mTOR antibody (Cat#380411, 1:1000 dilution), p62 antibody (Cat#380612, 1:2000 dilution), cleaved-caspase3 (Cat#341034, 1:1000 dilution) and LC3A/B antibody (Cat#306019, 1:1000 dilution) were purchased from Zhengneng Biotechnology Co., Ltd. (Chengdu, China). GAPDH (Cat#ET1601-4, 1:10000 dilution) and β-actin antibody (Cat#R1207-1, 1:10000 dilution) were purchased from Hangzhou Huaan Biotechnology Co., Ltd. (Zhejiang, China). The anti-mouse and anti-rabbit IgG, HRP-linked antibodies used in this study were purchased from Cell Signaling Technology (CST, Danvers, MA, USA), and the dilution ratio was 1:10,000. Bax antibody (Cat#60267-1, 1:1000 dilution) and Bcl-2 antibody (Cat#60178-1, 1:1000 dilution) were purchased from Proteintech.

2.3. Cell culture

U251 comes from a cell line preserved in the central laboratory of Guizhou Provincial People's Hospital (Guizhou, China); U87 cells purchased from Shanghai Fuheng Biotechnology Co., Ltd (Shanghai, China). LX-2 human hepatic stellate cells were obtained from the cell bank of the Chinese Academy of Sciences (Shanghai, China). They were cultured in Dulbecco's modified Eagle's medium (DMEM, Gibco, CA, China) supplemented with 10 % fetal bovine serum (FBS, Sijiqing, China) and incubated at 37 °C in a humidified environment under 5 % CO_2.

2.4. Cell proliferation assay

U251 and U87 cells (5×10^3 cells/well) were seeded in 96-well plates and treated with **FKL296** at different concentrations (0, 0.3125, 0.625, 1.25, 2.5, 5 μM) for 24,48,72h to assess cell proliferation,0.1 % DMSO as the control group, MTZ at different concentrations (0, 25, 50, 75, 100, 125 μM) for 48 h to assess cell proliferation,0.1 % DMSO as the control group. Next, the plate was placed under an inverted microscope to observe the status of the cells. MTT (Solarbio, Beijing, China) was added to each well, the cells were incubated for 4 h and the viability of cells was measured by reading the absorbance at 540 nm.

2.5. Toxicity assay

To determine the cytotoxicity of FKL296, LX-2 cells (3×10^3 cells/well) were seeded in 96-well plates for 24 h. Add **FKL296** with different concentrations to the final concentration of 0.3125, 0.625, 1.25, 2.5, 5 μM, DMSO as the control group, and incubate for 48 h. The selectivity index (SI) is commonly used to measure the safety of compounds. The calculation formula is: SI value of a compound = IC50 value of the compound to normal cells/IC50 value of the compound to tumor cells. The SI value indicates that a compound can inhibit tumor cells without damaging normal cells. The larger the SI value, the better the anti-tumor activity of the compound, and the lower its cytotoxicity to normal cells (Jamsheena et al., 2016).

2.6. Migration and invasion assay

The effect of **FKL296** on migration of U87 and U251 cells was assessed using the transwell inserts. Cells (1×10^4 cells/well) were resuspended in 200 μL medium without FBS, and added into the upper chamber, while the lower chamber was filled with 600 μL DMEM containing 10 % FBS, and the cells were incubated at 37 °C for 48 h. The invasion assay was performed also using transwell inserts, in which the membrane at the bottom of the insert was coated with Matrigel (1:7 dilution) (Corning Biocoat, USA), while the subsequent steps were the same as the migration assay. Migrated and invaded cells were fixed with 4 % paraformaldehyde, stained with 1 % crystal violet and photographed using an inverted microscope.

2.7. Apoptosis assay

U87 and U251 cell density was adjusted to 1×10^5 cells/well seeded in 6-well plates, and treated with different concentrations of **FKL296** for 48 h. Next, Hoechst333258 was added to each well, and incubated in the dark for 30 min, then the cells were washed twice with PBS, treated with fluorescence quenching blocking solution, and observed using an inverted microscope. A FITC Annexin V Apoptosis Detection Kit (Yi Shan biological, Shanghai, China) was used to assess apoptosis. U87 and U251 cells were seeded into 6-well culture plates for 24 h and treated with 1, 2 and 4 μM **FKL296** for 48 h, 0.1 % DMSO as the control group. Next, cells were harvested, and washed with PBS followed by the addition of 5 μL Annexin V-FITC and 5 μL PI for 15 min. Subsequently, apoptotic U87 and U251 cells were detected and quantified using flow cytometry.

2.8. Acridine orange (AO) and monodansylcadaverine (MDC) staining

U87 and U251 cells were seeded into a 6-well culture plate for 24 h and treated with 0, 1, 2, and 4 μM **FKL296** for 48 h, 0.1 % DMSO as the control group. Cells were collected according to the instructions, MDC (Cellular autophagic staining assay kit (Solarbio, Beijing, China) was incubated for 30 min in the dark, and AO (AO fluorescence staining reagent kit (Solarbio, Beijing, China)) for 15 min. Cells were photographed using an inverted microscope.

2.9. Kinase panel

The concentration of **FKL296** dissolved in DMSO compound mother liquor is 10 mM. The mother liquor of the compound is diluted to a concentration of 1mMand the positive control drug is also diluted to a concentration of 1 mM. During the experiment, **FKL296** detected a concentration of 10 μM. Add 2 × ATP, 2 × substrate solution, and 2 × kinase are prepared for kinase determination; Take 50 nl of compound into a 384 well plate and add 2 × kinase 2.5 μL. Incubate at room temperature for 10 min; Add 2 × ATP and 2 × substrate solution 2.5 μL. Incubate at room temperature for 60 min; Add antibodies and streptavidin to the 384 well plate; Incubate at room temperature for 60 min, use an enzyme-linked immunosorbent assay to detect fluorescence, with 665 nm/620 nm as reference data.

%Inhibition = 100 % − (composite positive control)/(negative control positive control) * 100 %.
Positive control: Average data of positive control (**FKL296** (10 μ M)).
Negative control: Average data of negative control (1 % DMSO).

2.10. Bioinformatics analysis

The gene expression profile interactive analysis (GEPIA) database and UALCAN analysis tool were used to evaluate the expression of SGK1, SGK2, and SGK3 in tumors, and the correlation between them and the overall survival and progression-free survival of GBM patients was also evaluated by the survival analysis module of GEPIA. STRING was used to analyze functional protein binding networks, Kyoto Encyclopedia of Genes and Genomes (KEGG) was used to assess pathway enrichment analyses.

2.11. Gene overexpression assay

A plasmid containing the SGK1 gene (Hunan Keai Medical Equipment Co., Ltd, Hunan, China) was used to assess the autophagy induced by SGK1 overexpression in U87 and U251 cells. The corresponding empty plasmid was used as a control. The overexpression plasmid was transfected into 293T cells, which were incubated for 48 h. Next, the virus solution was collected, and the titer was determined. U87 and U251 cells were seeded in 6-well plates and incubated at 37 °C overnight to let them adhere to the bottom. Virus solution and DMEM were added at a ratio of 1:1 and the cells were incubated for 24 h. Then the medium with the virus was replaced with fresh medium, and cells were incubated for 48 h. Next, cells were selected using puromycin (3 μg/mL) to obtain a stable cell line with SGK 1 overexpression. Total protein was extracted, the presence of overexpression was determined, and stable cell lines were used for further experiments.

2.12. Cellular thermal shift assay (CETSA)

CETSA-WB experiments were performed to further confirm the targeting of FKL-296 to SGK1. Cells were treated with FKL-296 (10 μM) for 2 h and then, washed twice with cold PBS. Subsequently, the cells were lysed 30 min using RIPA buffer containing a mixture of protease and phosphatase inhibitors. After centrifugation (15000 g, 20 min, 4 °C), proteins were collected, extracted, and divided into 8 equal parts. They were heated at 37, 40 45, 50, 55, 60, 65, and 70 °C for 3 min, then cooled at 4 °C for 3 min, and the supernatant was incubated with 1× loading buffer at 100 ℃ for 10 min. Protein expression was assessed using Western blotting.

2.13. Western blot

Cells were lysed using RIPA buffer (CoWin Biosciences, Beijing, China) containing protease inhibitor cocktail and phosphatase inhibitor cocktail (CWBIO, Beijing, China) on ice for 30 min. The supernatant was collected after centrifugation at 12,000 × g for 15 min and 4 °C. Proteins were separated by sodium dodecyl sulfate polyacrylamide gel electrophoresis (SDS-PAGE) and transferred into polyvinylidene fluoride (PVDF) membrane, which was blocked using 5 % bovine serum albumin (BSA) for 2 h. Subsequently, the membrane was incubated overnight at 4 °C with primary antibodies, followed by mouse or rabbit IgG secondary antibodies coupled to horseradish peroxidase (HRP) at room temperature for 1 h, then fixed with 4 % paraformaldehyde, and stained with 2 % crystal violet.

2.14. Animal experiments

Animal experiments were performed in accordance with the guideline of the Guizhou Medical University of the Animal Care Committee and the Key Laboratory of Natural Products Chemistry (license approval number: SYXK (Qian) 2018-0001). A total of 40 male BALB/C nude mice (18–22 g), 4 weeks old, were purchased from Chongqing Tengxin Biotechnology. U87 cells with stable growth were resuspended in physiological saline solution at a density of 1×10^6 /0.1 mL. When the tumor volume reached approximately 100 mm^3, the mice were randomly divided into a model group and two drug treatment groups (5 mg/kg and 20 mg/kg) and treated with **FKL296** every other day. The weight and volume of the tumor were recorded every 3 days. Mice were euthanized after 15 days and the heart, liver, spleen, lungs, kidneys, and tumor were removed and weighed. Immunohistochemical staining and hematoxylin-eosin staining of tissue sections were performed by Wuhan Servicebio.

2.15. Statistical analysis

Statistical analysis was performed using IBM SPSS version 21.0 and GraphPad Prism 8.0. The difference between two groups was evaluated using *t*-test, and the difference among more than two groups was evaluated using one-way analysis of variance (ANOVA). Results were presented as mean ± standard deviation (SD) of at least three independent experiments. A value of $P < 0.05$ is considered statistically significant.

3. Results

3.1. FKL296 inhibited the growth of GBM cells

FKL296 is a type of quinoline derivative. The molecular formula of **FKL296** is $C_{30}H_{30}F_3N_5O_4$ and the molecular weight is 581.60 KDa. The structural formula of **FKL296** is shown in Fig. 1A. To determine whether **FKL296** inhibits the activity, migration, and invasion of GBM, U87 and U251 cells were incubated with increasing concentrations of **FKL296** and examined through different assays. We performed MTT assays, in which U87 and U251 cells were treated with **FKL296** for 24, 48 and 72 h. The half-maximal inhibitory concentrations (IC_{50}) in U87 and U251 cells were 1.71 μM and 1.55 μM, respectively, for 48 h. In addition, after incubating with TMZ for 48 h, we found that the IC_{50} values of U87 and U251 were 97.61 μM and 68.96 μM, respectively. Therefore, MTT assays showed that **FKL296** inhibited the growth of GBM cells (Fig. 1B, S1A). The inverted microscope results of GBM cells treated with **FKL296** showed a decrease in cell count (Fig. 1C). To verify the toxic effect of **FKL296** on GBM, we used the selectivity index for toxicity evaluation. According to Table S1, the SI values of U87 and U251 are 1.45 and 1.60, respectively, indicating that **FKL296** may have potential toxicity (Fig. S1B). It has been demonstrated in studies that the migration and invasion potential play a crucial role in the mortality rates of patients with GBM. The effect of **FKL296** on the migration and invasion of GBM cell was examined using a Transwell assay. The results showed that **FKL296** significantly reduced the migration and invasion of U87 and U251 cells in a dose-dependent manner, the number of cells passing through the chamber membrane is significantly reduced after treatment with 4 μM **FKL296** (Fig. 1D). In summary, **FKL296** effectively inhibits the proliferation, migration, and invasion of GBM cells.

3.2. FKL296 inhibited tumor proliferation in nude mice

The treatment results of **FKL296** on BALB/c nude mouse GBM tumor model showed significant differences between the high-dose group and the model group at the end of treatment (Fig. 2A and B, $P < 0.01$), indicating that the high-dose group of **FKL296** significantly inhibited tumor growth. No significant difference in tumor volume was observed between **FKL296** and the model group after 6 days of treatment. The tumor volume of the high-dose group was statistically significant than that of the model group from day 9 onward ($P < 0.01$). The tumor volume in mice that did not receive **FKL296** treatment was approximately 600 mm^3, while the tumor volume in the high-dose treatment group was approximately 200 mm^3 (Fig. 2C). Compared with the model group, after treatment with **FKL-296** (20 mg/kg), the weight of mice slightly decreased, but there was no statistically significant difference in weight (Fig. 2D). In order to test the safety of **FKL296** against glioblastoma, we weighed the hearts, livers, spleens, lungs, and kidneys of the **FKL296** 5 mg/kg and 20 mg/kg treatment groups and the model group. The results showed that the organ weights of the mice treated with **FKL296** did not show significant changes compared to the model group (Fig. 2E), Subsequently, we stained the mouse organs with HE tissue slices, which is no significant difference in the morphology of each organ after **FKL296** treatment compared with the model group (Fig. 2F). These results demonstrated that **FKL296** exerted a low toxicity *in vivo*.

3.3. FKL296 induced apoptosis of GBM cells

The nuclear morphology of U87 and U251 cells showed significant changes after incubation with **FKL296** for 48 h, such as chromatin aggregates on one side of the nuclear membrane, cell contraction, DNA fragmentation, irregular cell shape, and separation (Fig. 3A). The treatment with 2 μM and 4 μM **FKL296** for 48 h (Fig. 3B) revealed that the percentage of early and late apoptosis significantly increased in U87 and U251 cells. The expression of proteins related to cell apoptosis (Fig. 3C) showed that caspase 3 and Bcl-2 were decreased, while that of cleaved- caspase 3 and Bax was increased (Fig. 3D). These results demonstrated that **FKL296** induced apoptosis in GBM cells.

3.4. FKL296 induced autophagy of GBM cells

After 48 h of treatment with **FKL296**, AO and MDC staining were performed to assess the potential induction of autophagy by **FKL296** in U87 and U251 cells. The results indicated that autophagosomes and lysosomes increased in U87 and U251 cells (Fig. 4A and B). The TME results showed that treatment with **FKL296** lead to an increase in the number of damaged organelles with double-membrane structure autophagosomes and autophagosomes (Fig. 4C). In addition, the expression of proteins related to cellular autophagy is revealed in Fig. 4D. One of the important markers of autophagy is the conversion of LC3I to LC3II, with an increase in LC3II/LC3I levels (Fig. 4E).

3.5. SGK1 is an important target of FKL296 in the treatment of glioblastoma

In order to investigate the potential targets of **FKL296** in the treatment of glioblastoma, the results of protein kinase profiling screening showed that DYRK4 and CaMK1α ranked in the top ten, followed by HER2, DAPK1, SGK2, PKD2, PKCβ1, SGK, SGK3, and AKT2 (Fig. 5A and B). Literature search shows that genes that affect cell apoptosis and autophagy in neurological diseases and are highly expressed in tumor tissues are mainly focused on the SGK family. SGK is a filament/threonine protein kinase consisting of SGK1, SGK2, and SGK3 (Sang et al., 2021, Cicenas et al., 2022), which regulate the apoptosis and autophagy in tumor cells.

The differential expression of SGK in GBM was searched in the GEPIA database (https://gepia.cancer-pku.cn/), and the results showed that only SGK1 expression was significantly higher in GBM, while the expression of SGK2 and SGK3 was not significantly different than that in normal tissues (Fig. 5C), In addition, the effect of the SGK family on the overall survival and progression-free survival of GBM patients was assessed and the results showed that SGK1, SGK2, and SGK3 had little effect on overall survival, low expression of SGK1 in progression-free survival brings more adverse disease-free survival, and high expression of SGK2 and SGK3 prevented treatment progression (Fig. 5D and E). Therefore, our speculation was that SGK1 might be a potential therapeutic target of **FKL296**.

The binding affinity of **FKL296** for SGK1 was simulated by molecular docking, showing that they had the best binding affinity of −10.2 kcal/mol (Fig. 5F). The targeted binding of **FKL296** to SGK1 in molecular docking was verified by CETSA. U87 and U251 cells treated with **FKL296** (10 μM) or DMSO were subjected to CETSA thermal pulse, and the results revealed that SGK1 possessed a significant thermal stability in the **FKL296** treated group. All the above results suggested that **FKL296** might target SGK1 to regulate apoptosis and autophagy in GBM (Fig. 5G and H).

3.6. FKL-296 induced autophagy via regulating the mTOR/FOXO3a pathway in GBM cells

A protein–protein interaction (PPI) network was initially constructed through the STRING database to investigate the biological role of SGK1, using SGK1 as the core. A total of 11 main nodes were present (Fig. 6A). KEGG pathway enrichment analysis showed that SGK1 was significantly enriched in signaling pathways related to cellular autophagy, including the FOXO signaling pathway, mTOR signaling pathway, MAPA signaling pathway, and PI3K/AKT signaling pathway (Fig. 6B). Besides genes that were mainly enriched in the FOXO signaling pathway and mTOR signaling pathway, SGK1 in the FOXO signaling pathway was mainly regulated by FOXO3a to regulate autophagy. Studies have shown that SGK1 has apoptosis-promoting effects by regulating FOXO3a, negatively regulates cell death by inhibiting FOXO3a activity, and under conditions

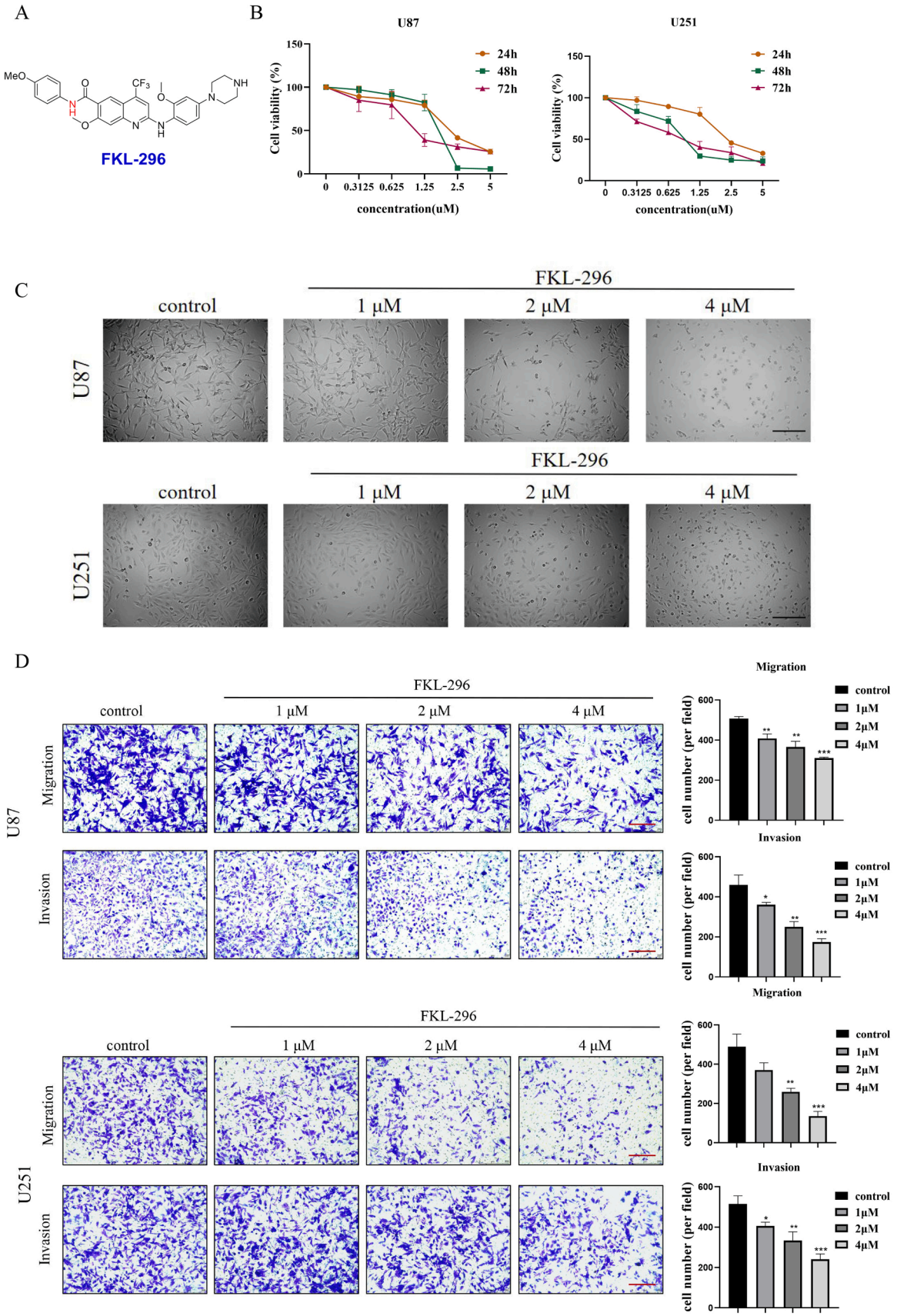

Fig. 1. FKL296 inhibited activity, migration, and invasion of GBM cells. (A) Structure of **FKL296**. (B) **FKL296** significantly inhibited the viability of GBM cells at 24, 48 and 72 h. (C) The morphological features of U87 and U251 cells treated with **FKL296**. (D) Transwell assays showed that **FKL296** inhibited the migration and invasion of U87 and U251cells. Scale bar = 250 μm. Control: DMSO used as a control. The data are expressed as the mean ± SD (n = 3). $^{*}P < 0.05$, $^{**}P < 0.01$, $^{***}P < 0.001$.

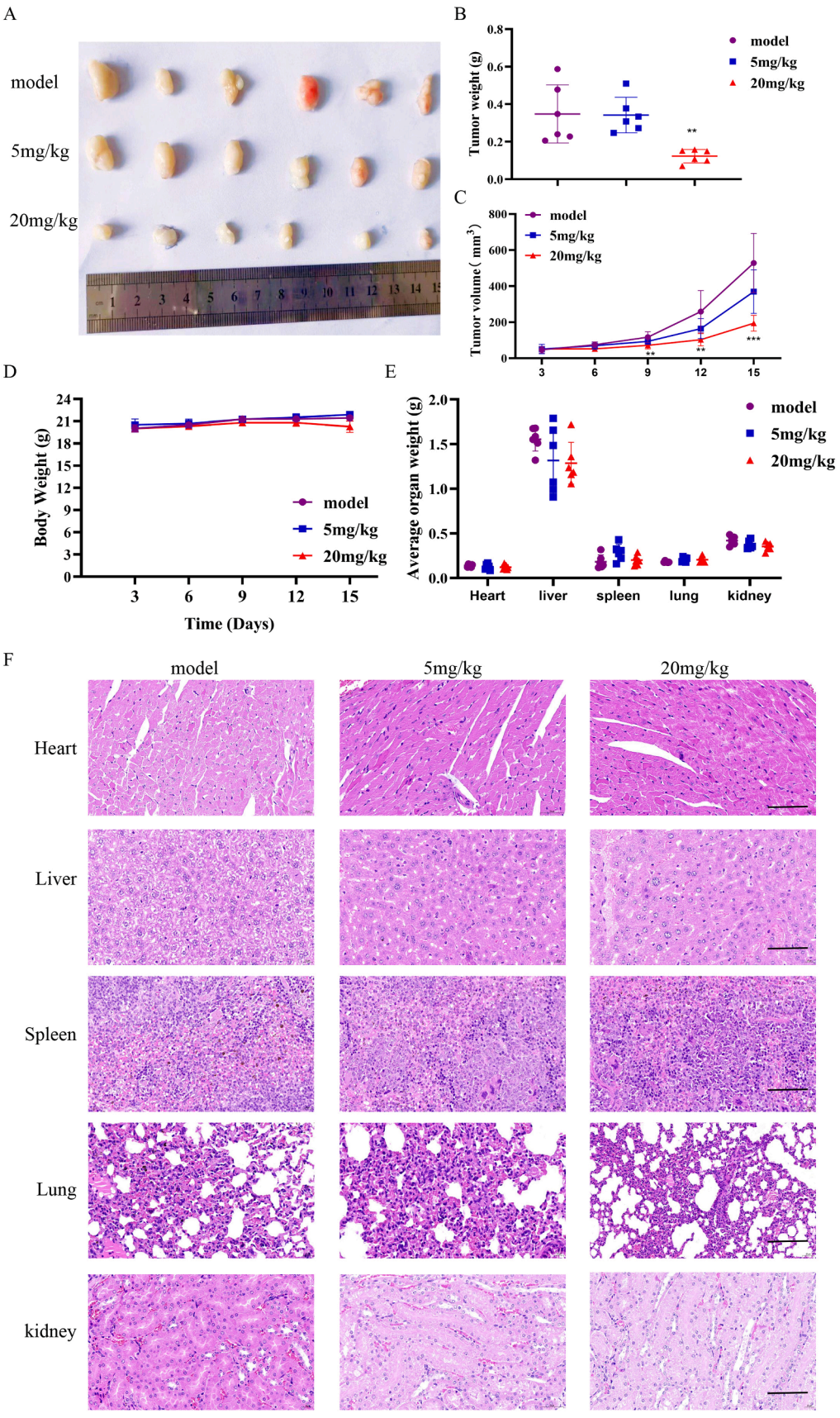

Fig. 2. FKL296 inhibited tumor proliferation in nude mice. (A) Tumor size; (B) Tumor weight; (C) Tumor volume (D) Body weight; (D) Organ weight. (E) Results of HE is staining in heart, liver, spleen, lung and kidney, scale bar = 250 μm. Data are expressed as mean ± SD (n = 6). $^{*}P < 0.05$, $^{**}P < 0.01$, $^{***}P < 0.001$.

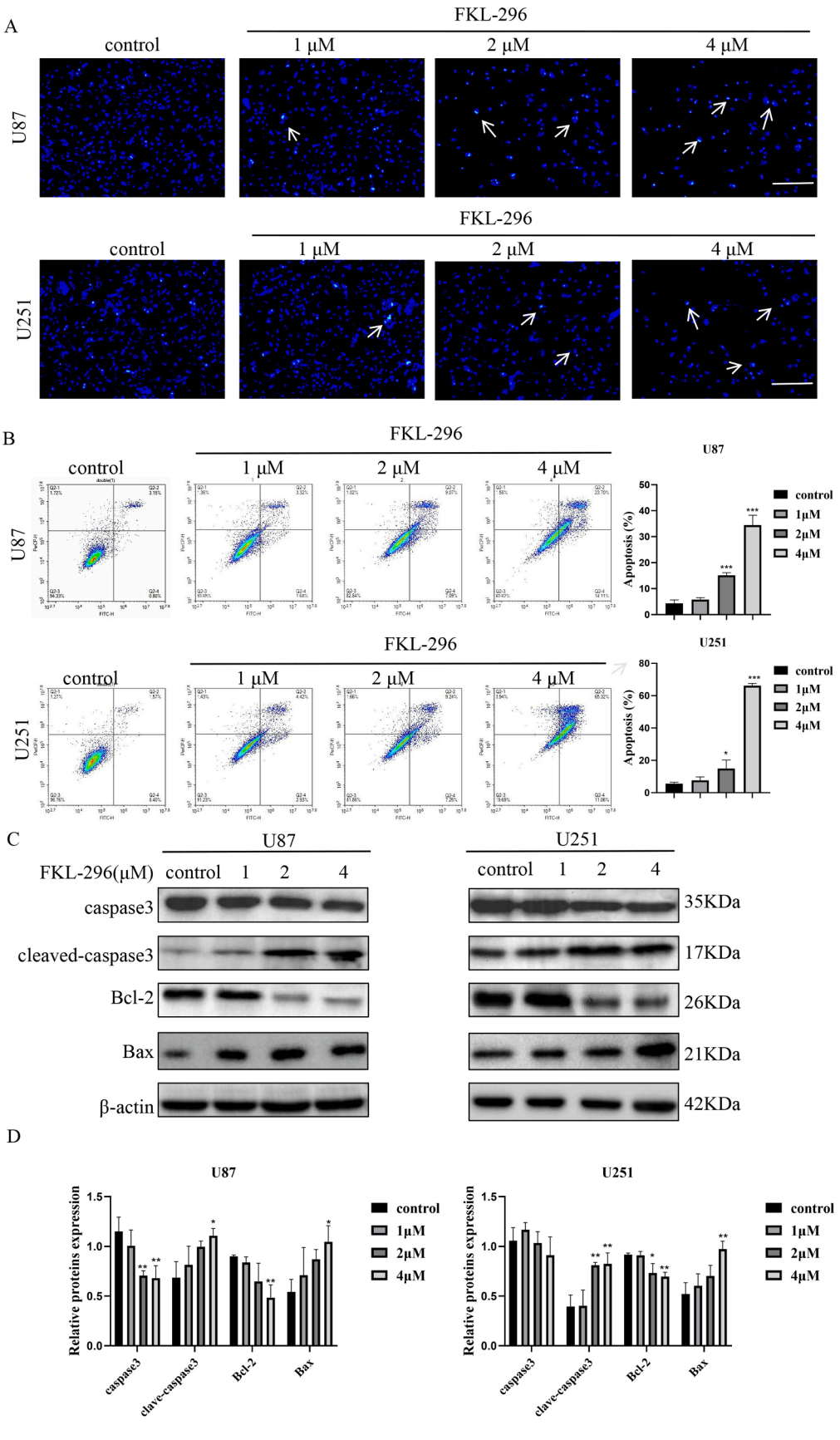

(caption on next page)

Fig. 3. FKL296 promoted GBM cells apoptosis. (A) Morphological changes in the nuclei of U87 and U251 cells treated with **FKL296**. The arrow represents chromatin aggregates on one side of the nuclear membrane, cell contraction, DNA fragmentation, irregular cell shape, and separation. Scale bar = 250 μm. (B) Flow cytometry using PI/Annexin V-FITC double staining showed that **FKL296** induced apoptosis in U87 cells at 48 h. (C) Western blot analysis for determining the expression levels of cleaved caspase3, Bax, and Bcl-2 proteins in U87 and U251 cells. (D) The expression of Bax and cleaved caspase3 was up-regulated, while that of caspase3 and Bcl-2 was reduced. Control: DMSO used as a control. The data are expressed as the mean ± SD (n = 3). $^{*}P < 0.05$, $^{**}P < 0.01$, $^{***}P < 0.001$.

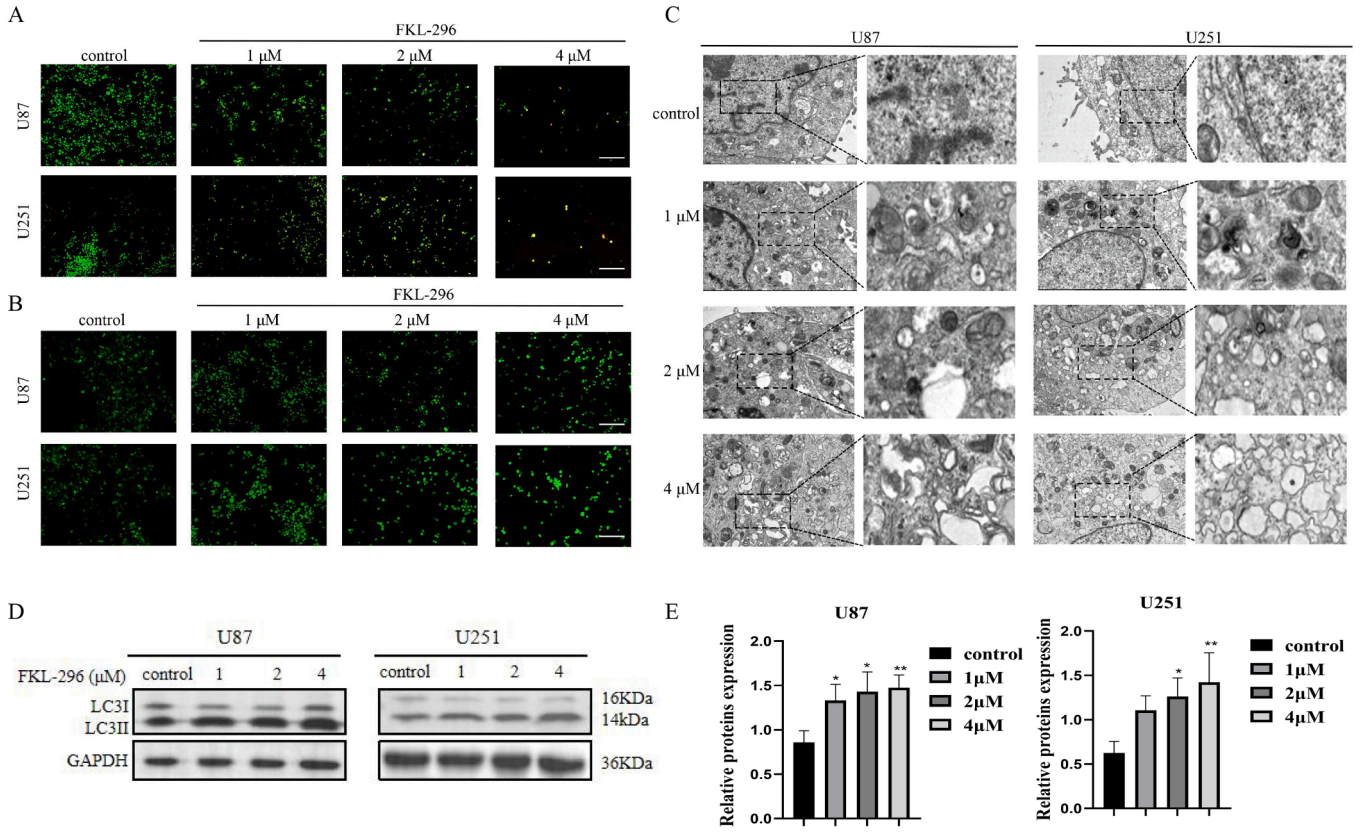

Fig. 4. FKL296 induced autophagy in glioblastoma. (A) AO staining; (B) MDC staining; (C) The submicroscopic structural morphology analysis was performed by transmission electron microscopy; (D) Proteins associated with autophagy in **FKL296**-treated U87 cells and U251 cells quantitated by Western blotting; (E) The expression of LC3II/LC3I was upregulated. Control: DMSO used as a control. The data are expressed as the mean ± SD (n = 3). $^{*}P < 0.05$, $^{**}P < 0.01$, $^{***}P < 0.001$.

above the apoptotic threshold, FOXO3a promotes autophagy-mediated cell death (Ortuso et al., 2014). Therefore, our speculation was that **FKL296** targets SGK 1 to activate autophagy and apoptosis of GBM through the FOXO3a/mTOR pathway. The results (Fig. 6C) demonstrated that the expression of mTOR and p62 protein decreased, while the expression of FOXO3a increased with increasing **FKL296** concentrations (Fig. 6D). Moreover, Immunohistochemical analysis showed that mTOR was downregulated, while FOXO3a was upregulated in the tumors treated with **FKL296**, which was consistent with the cellular results (Fig. 6E). Overall, these results demonstrated that **FKL296** targeted SGK1 to activate the FOXO3a/mTOR pathway to induce the autophagy and apoptosis of GBM.

3.7. SGK1 overexpression reduced FKL296-induced autophagy in GBM cells

To further investigate the role of SGK1 in **FKL296** induced autophagy in GBM cells, we transfected U87 and U251 cells with an SGK1 overexpression plasmidto increase the expression level of SGK1. As a result, the experimental group showed stronger cell viability compared to the control group (Fig. 7A and B). In addition, we evaluated the expression of proteins related to cell autophagy through western blotting, In the absence of drug treatment, the expression of LC3II/LC3I and FOXO3a in the oeSGK1 group decreased compared to the oeCtrl group, while the expression of p62 and mTOR increased. However, after **FKL296** treatment, the expression of LC3II/LC3I and FOXO3a in the oeSGK1 group increased compared to the oeSGK1 group (without drug treatment), while the expression of p62 and mTOR in the oeSGK1 group decreased compared to the oeSGK1 group (without drug treatment) (Fig. 7C and D).These results indicate that oeSGK1 inhibits autophagy, while FKL296 effectively reverses autophagy.

3.8. FKL296 aggravated autophagy induced by SGK1 inhibitor SI113 in GBM cells

SI113 is a small molecular weight membrane permeant compound, working as an inhibitor of SGK1-mediated pathways (D'Antona et al., 2015). In addition, studies have shown that SI113 was used in various preclinical studies on GBM, ovarian cancer, and colon cancer cells as a potential chemotherapeutic agent (Abbruzzese et al., 2017, D'Antona et al., 2019). It was reported that SI113 in GBM cells had a IC_{50} range of 9—11 μM (Ortuso et al., 2014), therefore, 10 μM SI113 was used in our experiments. The MTT results indicated that **FKL296** combined with SI113 significantly inhibited the viability of U87 and U251 cells. (Fig. 8A). To further explore whether SI113 and FKL-296 induced autophagy in GBM cells, the treatment of U87 and U251 cells with SI113 and **FKL296** resulted in a decrease in mTOR and p62 protein expression and an increase in LC3II/LC3I and FOXO3a expression (Fig. 8B and C).

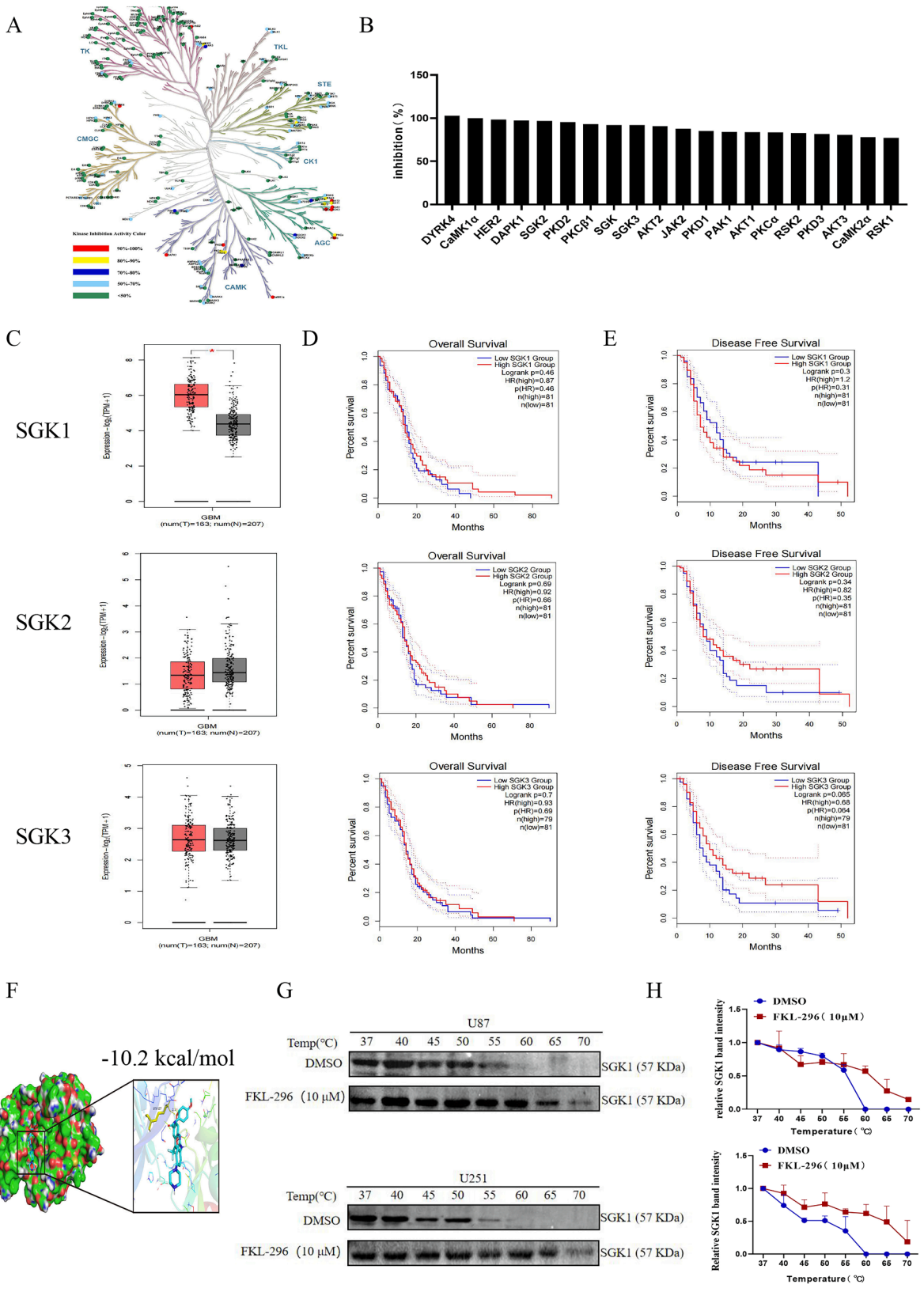

Fig. 5. SGK1 is an important target of FKL296 in the treatment of glioblastoma. (A,B) Protein kinase profiling to screen for potential targets of **FKL296** in glioblastoma. (C) The GEPIA database was used to verify the expression of SGK1, SGK2 and SGK3 in GBM tissues and adjacent normal tissues.T (red): tumor, N (grey): normal. (D,E) Survival analysis of SGK1, SGK2 and SGK3. (F) Molecular docking visualization model of compound **FKL296** with the protein SGK1. (G,H) A CETSA was used to verify the binding affinity of **FKL296** to the SGK1 protein. Control: DMSO used as a control. The data are expressed as the mean ± SD (n = 3). $^{*}P < 0.05$, $^{**}P < 0.01$, $^{***}P < 0.001$. (For interpretation of the references to colour in this figure legend, the reader is referred to the web version of this article.)

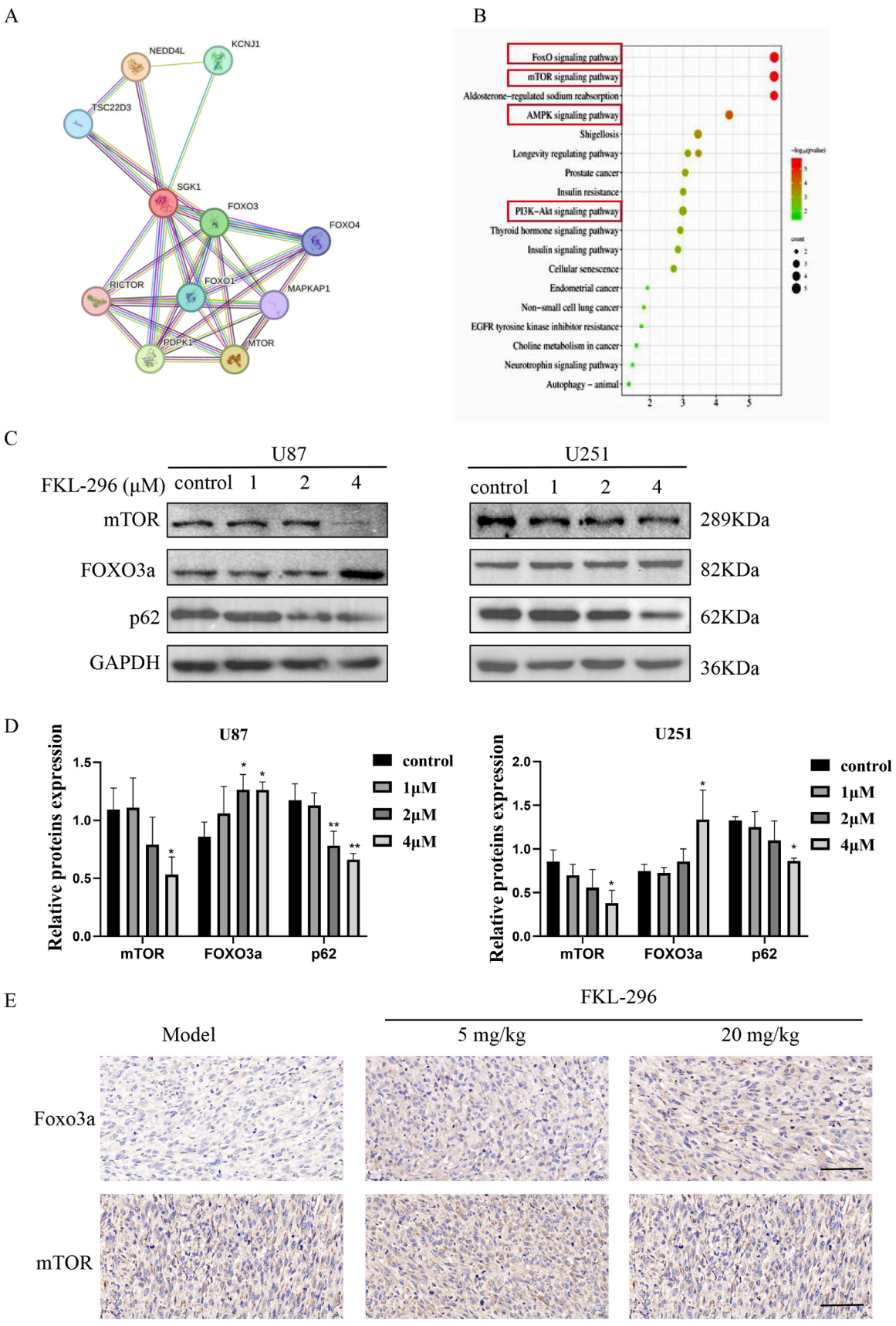

Fig. 6. FKL-296 induced autophagy via regulating the mTOR/FOXO3a pathway in GBM cells. (A) PPI network of SGK1. (B) KEGG analysis. (C) Proteins associated with autophagy in **FKL296**-treated U87 cells and U251 cells quantitated by Western blotting (D) The expression of FOXO3a was up-regulated, while p62 and mTOR were reduced. (E) Immunohistochemical analysis for evaluating FOXO3a and mTOR expression levels in tumors from mice in the model and **FKL296** groups (scale bar: 250 μm). Control: DMSO used as a control. The data are expressed as the mean ± SD (n = 3). $^{*}P < 0.05$, $^{**}P < 0.01$, $^{***}P < 0.001$.

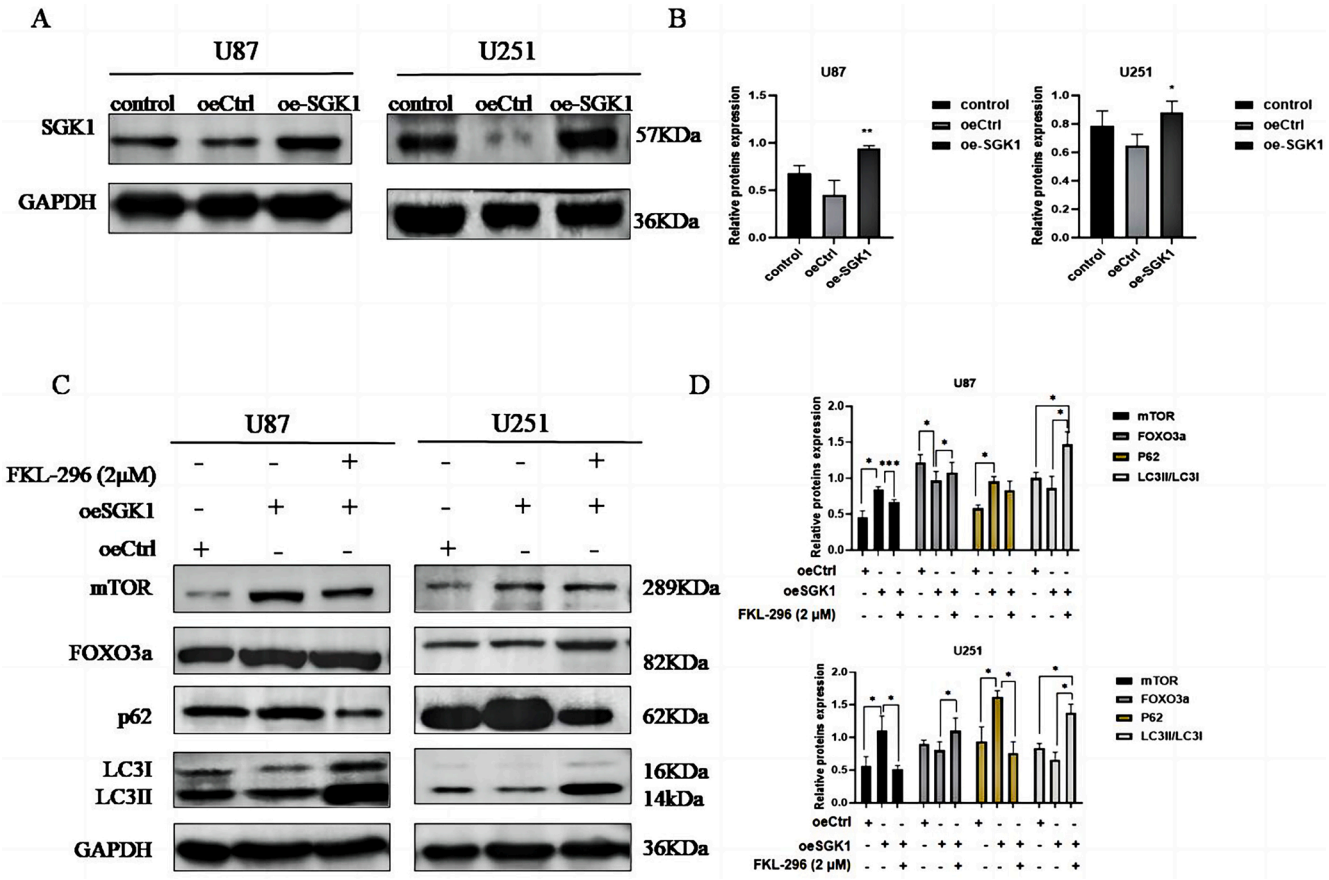

Fig. 7. SGK1 overexpression reduced FKL296-induced autophagy in GBM cells. (A, B) SGK1 Expression was significantly upregulated. (C, D) Proteins associated with autophagy by western blotting. Control: DMSO used as a control, oeCtrl:It represents the wild type, Oe-SGK1: It represents overexpression of SGK1 type. Results are expressed as mean ± SD (n = 3). $^{*}P < 0.05$, $^{**}P < 0.01$, $^{***}P < 0.001$.

The detection of autophagy related proteins in GBM cells overexpressing SGK1 showed that In the absence of drug treatment, the expression of LC3II/LC3I and FOXO3a in the oeSGK1 group decreased compared to the oeCtrl group, while the expression of p62 and mTOR increased. However, after the combination of **FKL296** and SI113, the expression of LC3II/LC3I and FOXO3a in the oeSGK1 group increased again compared to the oeSGK1 group (without drug treatment), while the expression of p62 and mTOR in the oeSGK1 group decreased compared to the oeSGK1 group (without drug treatment) (Fig. 8D and E), indicating that **FKL296** aggravated autophagy induced by SGK1 inhibitor SI113 in GBM cells.

4. Discussion

GBM is one of the most invasive cancers and has a poor prognosis. So far, TMZ is an oral alkylating agent with good CNS penetration, and it is the only chemotherapy drug approved for the treatment of GBM (Fernandes et al., 2017). However, long-term use of TMZ can lead to drug resistance in patients (Jia et al., 2023). In this study, we found that **FKL296** significantly inhibited the proliferation, migration, and invasion of GBM cells. This compound induces apoptosis and autophagy in GBM cells and may inhibit the development of tumors *in vivo*. We found that SGK1 has a strong binding ability through protein kinase profiling and molecular docking. According to the CETSA results, **FKL296** can target and bind to SGK1. In order to understand the biological role of SGK1, bioinformatics analysis revealed that SGK1 may regulate autophagy and apoptosis in cancer through the mTOR/FOXO3a signaling pathway. However, overexpression of SGK1 inhibited autophagy, which was effectively reversed by **FKL296**. The SGK1 inhibitor SI113 can induce autophagy in GBM cells. **FKL296** can inhibit tumor growth and has good safety in in *in vivo*. We elucidated the potential mechanism of **FKL296** targeting SGK1 to induce autophagy and apoptosis in GBM through the FOXO3a/mTOR pathway (Fig. 9).

Natural products and their derivatives are a rich source of new small molecule compounds for cancer treatment (Li et al., 2017). Our previous research has confirmed the synthesis of a new anti-cancer compound FKL296 by introducing fluorinated functional groups into different parts of the natural product quinoline.We reported that **FKL296** can inhibit the activity of GBM *in vivo* and *in vitro*, and demonstrated its potential mechanism. We calculated that IC_{50} U87 cells were 1.71 μM and U251 cells were 1.55 μM, and our results showed that FKL296 has good activity.

Serum and glucocorticoid-regulated kinases (SGKs) are members of the serine/threonine kinase AGC (PKA-, PKG-, PKC-related) family, and are among the most evolutionarily conserved groups of protein kinases (Arencibia et al., 2013). The SGK family consists of three distinct but highly homologous isoforms (SGK1, SGK2, and SGK3) that are generated from three different genes located on different chromosomes (Lang et al., 2001). SGK1 plays an important role in predicting the prognosis of cancer patients. For example, in patients with glioblastoma multiforme, fewer SGK1 gene copy number segments are significantly associated with low survival, while increased SGK1 copy number segments cause an associated increase in median overall survival (Lehrer et al., 2018). High expression of SGK1 can reduce the overall survival of cancer patients and has a strong prognostic value. SGK1 has multiple functions in cancer, including proliferation (Liang et al., 2017), apoptosis (Sherk et al., 2008), invasion (Tian et al., 2017), migration (Schmidt et al., 2012), and cancer metabolism (Matschke et al., 2016).

Our data indicates that **FKL296** induces apoptosis in glioblastoma,

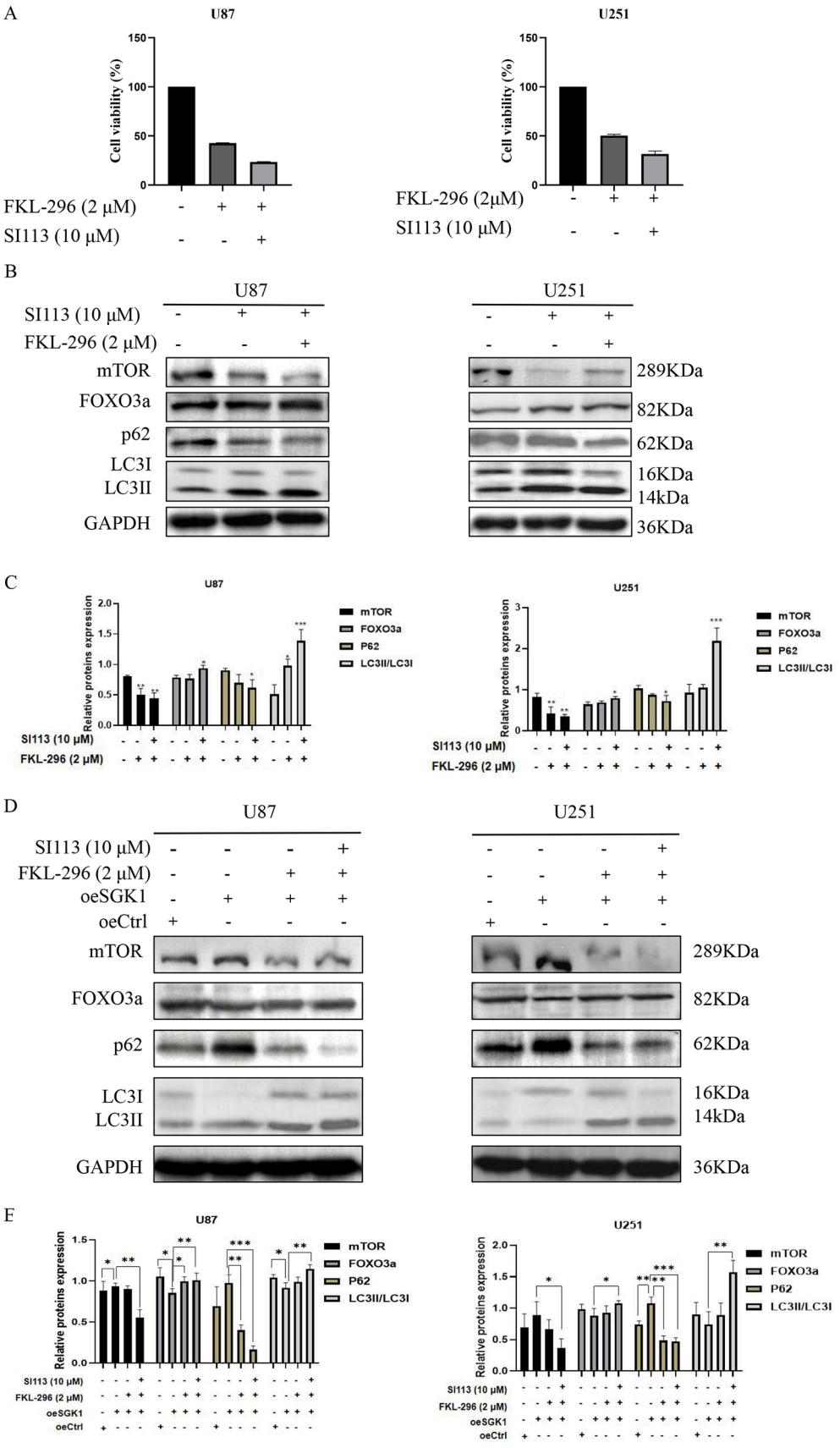

Fig. 8. FKL296 aggravated autophagy induced by SGK1 inhibitor SI113 in GBM cells. (A)MTT assay to verify the activity of si113 in U87 and U251 cells. (B) and (C) Effects of **FKL296**, and SI113 on autophagy in GBM cells. (D) and (E) Effects of **FKL296**, and SI113 on autophagy in GBM-overexpression cells. Control: DMSO used as a control, oeCtrl:It represents the wild type, Oe-SGK1: It represents overexpression of SGK1 type. The data are expressed as the mean ± SD (n = 3). $^{*}P < 0.05$, $^{**}P < 0.01$, $^{***}P < 0.001$.

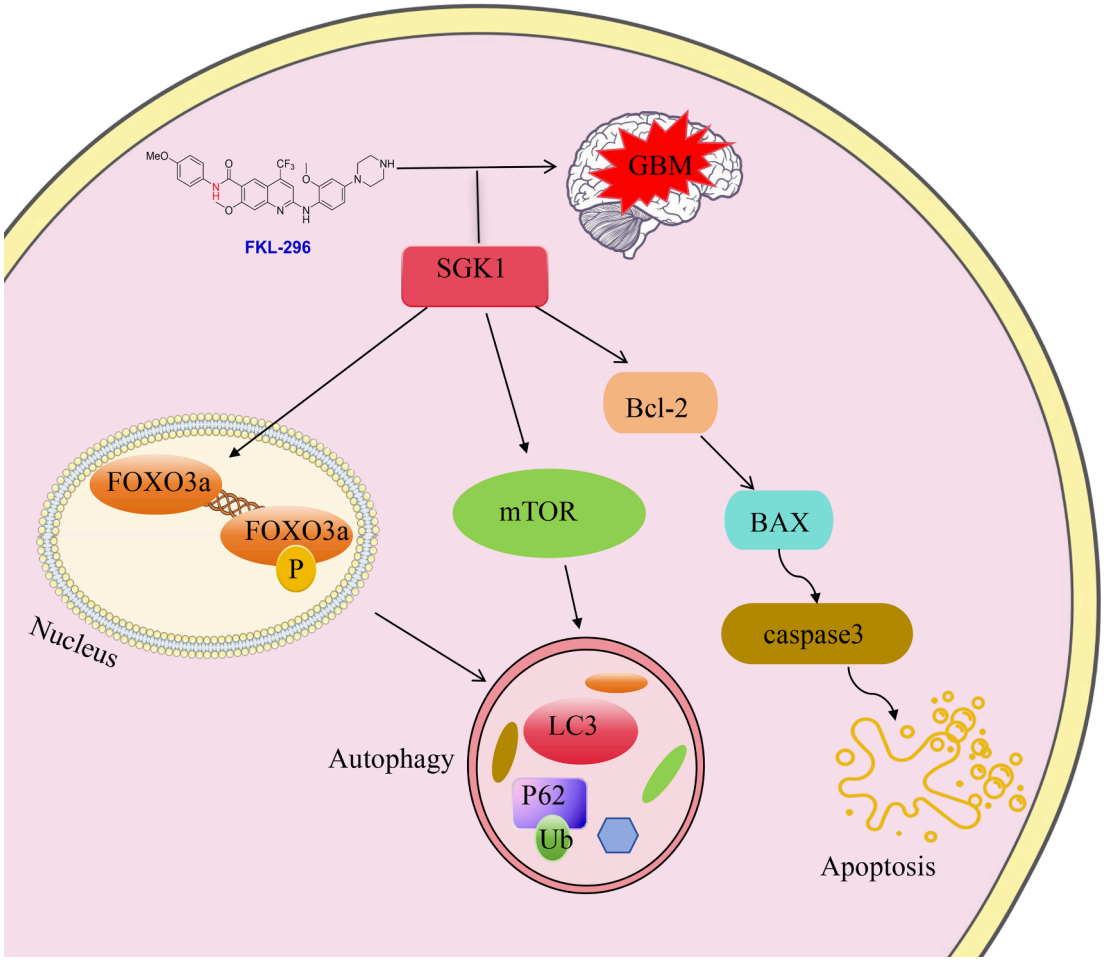

Fig. 9. FKL296 regulates autophagy and apoptosis in glioblastoma cells by targeting SGK1.

with decreased expression of Bcl-2 and increased expression of Bax in treated GBM cells. Research has shown that mitochondrial dysfunction leads to the activation of caspase-3 and subsequent PARP cleavage (Cui et al., 2018). In GBM cells treated with **FKL296**, the expression of Bcl-2 was also reduced, while the expression of Bax was increased, resulting in a decrease in cleaved caspase3/caspase3. Autophagy is a key homeostatic pathway that facilitates the degradation and recycling of cellular material (Klionsky et al., 2021). Autophagy plays an important role in both internal and external factors of tumor growth (Debnath et al., 2023). Previous studies have shown a negative correlation between p62 and selective autophagic degradation, and p62 can be degraded by directly binding to LC3II in autolysts (Xiang et al., 2021). Therefore, the levels of p62 and LC3II can serve as good indicators of autophagy (Klionsky et al., 2016). We examined the effect of **FKL296** on autophagy in GBM cells and found that **FKL296** may induce autophagy in GBM through the FOXO3a/mTOR signaling pathway. Studies have shown that autophagy is involved in the degradation of misfolded and unfolded protein structures, but can only reach a certain threshold. Beyond this threshold, autophagic proteins can participate in the apoptotic mechanism to regulate the apoptotic cascade reaction, without activating the entire autophagy process. In addition, there may be a synergistic effect between autophagy and cell apoptosis. The autophagy regulatory transcription factor FOXO3a itself is flipped by basal autophagy, forming a potential feedback loop. After autophagy inhibition, an increase in FOXO3a stimulates the transcription of pro apoptotic BBC3/PUMA genes, leading to cell apoptosis sensitization (Fitzwalter et al., 2018). Foglio et al.'s research has shown that the expression of proteins such as LC3, Beclin-1, and Atg7 increases, while the expression of Bax, Bcl-2, Caspase 3, and mTOR decreases. HMGB1 induces autophagy in diseases (Foglio et al., 2017). Autophagy plays a dual role in the occurrence and development of cancer, and molecular crosstalk between autophagy and cell apoptosis is a complex process (Das et al., 2021). However, the relationship between autophagy and cell apoptosis has not yet been revealed, and further exploration is needed.

In summary, **FKL296** can target SGK1 and induce autophagy in glioblastoma through the FOXO3a/mTOR signaling pathway. However, this article also has some drawbacks, such as whether the increase of **FKL296** will lead to TMZ chemical sensitivity, and the effects of **FKL296** on mouse brain tissue. In addition, we will further investigate the mechanism of **FKL296** in the treatment of GBM, these are all areas that we need to explore and research in the future. We conducted preliminary research and exploration on the mechanism of action of the novel **FKL296** in the treatment of GBM, laying the foundation for **FKL296** as a potential therapeutic drug for GBM.

5. Conclusions

The anticancer compound **FKL296** is composed of quinoline derivatives with fluorinated functional groups. This study demonstrated through a series of *in vitro* and *in vivo* experiments that **FKL-296** can effectively inhibit the growth of glioblastoma and is relatively safe and low toxicity. In addition, our research results confirm that **FKL296** can induce apoptosis and autophagy in glioblastoma, and can target SGK1 to activate autophagy in GBM cells through the mTOR/FOXO3a pathway. In summary, all these results suggest that **FKL296** may become a new hope for the treatment of glioblastom.

Ethics statement

The animal study was reviewed and approved by the Ethics Committee of Guizhou University. NO: EAE-GZU-2023-E056.

CRediT authorship contribution statement

Yu-feng Xiong: Writing – original draft, Conceptualization, Methodology, Formal analysis, Investigation. **Cheng Li:** Writing – review & editing, Investigation. **Jia Yu:** Writing – review & editing, Investigation. **Xiaozhong Chen:** Writing – review & editing, Investigation. **Sha Cheng:** Writing – review & editing, Investigation. **Xin-yu Liu:** Writing – review & editing, Investigation. **Bi-xue Xu:** Conceptualization, Funding acquisition, Resources, Supervision, Writing – review & editing. **Xiao Hu:** Conceptualization, Funding acquisition, Resources, Supervision, Writing – review & editing. **Guang-can Xu:** Conceptualization, Funding acquisition, Resources, Supervision, Writing – review & editing. **Heng Luo:** Conceptualization, Funding acquisition, Resources, Supervision, Writing – review & editing.

Declaration of Competing Interest

The authors declare that they have no known competing financial interests or personal relationships that could have appeared to influence the work reported in this paper.

Acknowledgments

We are grateful for the financial support from the National Natural Science Foundations of China (82260675), the Department of Science and Technology of Guizhou Province (No. QKHZYD[2022]4015, QKHJC-ZK-ZK[2021] normal 463), the Natural Science Foundation of Guizhou Province (No. QKHJC-ZK[2021]YB07, No. QKHJC-ZK[2022] ZD031), the Guizhou Province "Hundred" Level Innovative Talent Training Project (No. QKHPTRC-GCC [2022]034-1), the Natural Science Foundation of Guizhou Medical University (No. 21NSFCP42), and the Higher Education Scientific Research Project of the Department of Education of Guizhou Province (No. QJJ[2022]184).

Appendix A. Supplementary data

Supplementary data to this article can be found online at https://doi.org/10.1016/j.arabjc.2024.105909.

References

Abbruzzese, C., Catalogna, G., Gallo, E., di Martino, S., Mileo, A.M., Carosi, M., Dattilo, V., Schenone, S., Musumeci, F., Lavia, P., Perrotti, N., Amato, R., Paggi, M. G., 2017. The small molecule SI113 synergizes with mitotic spindle poisons in arresting the growth of human glioblastoma multiforme. Oncotarget 8 (67), 110743–110755. https://doi.org/10.18632/oncotarget.22500.

Arencibia, J.M., Pastor-Flores, D., Bauer, A.F., Schulze, J.O., Biondi, R.M., 2013. AGC protein kinases: from structural mechanism of regulation to allosteric drug development for the treatment of human diseases. BBA 1834 (7), 1302–1321. https://doi.org/10.1016/j.bbapap.2013.03.010.

Blaskovich, M.A.T., 2019. Quinolone antibiotics. Medchemcomm. https://doi.org/10.1039/c9md00120d.

Butler, M., et al., 2020. MGMT status as a clinical biomarker in glioblastoma. Trends Cancer. 6 (5), 380–391. https://doi.org/10.1016/j.trecan.2020.02.010.

Cicenas, J., Meskinyte-Kausiliene, E., Jukna, V., Rimkus, A., Simkus, J., Soderholm, D., 2022. SGK1 in cancer: biomarker and drug target. Cancers (basel). 14 (10), 2385. https://doi.org/10.3390/cancers14102385.

Cui, L., Bu, W., Song, J., Feng, L., Xu, T., Liu, D., et al., 2018. Apoptosis induction by alantolactone in breast cancer MDA-MB-231 cells through reactive oxygen species-mediated mitochondrion-dependent pathway. Arch. Pharm. Res. 41 (3), 299–313. https://doi.org/10.1007/s12272-017-0990-2.

D'Antona, L., Amato, R., Talarico, C., et al., 2015. SI113, a specific inhibitor of the Sgk1 kinase activity that counteracts cancer cell proliferation. Cell. Physiol. Biochem. 35, 2006–2018. https://doi.org/10.1159/00037.

D'Antona, L., Dattilo, V., Catalogna, G., et al., 2019. In preclinical model of ovarian cancer, the SGK1 inhibitor SI113 counteracts the development of paclitaxel resistance and restores drug sensitivity. Transl. Oncol. 12 (8), 1045–1055. https://doi.org/10.1016/j.tranon.2019.05.008.

Das, S., Shukla, N., Singh, S.S., Kushwaha, S., Shrivastava, R., 2021. Mechanism of interaction between autophagy and apoptosis in cancer. Apoptosis 26 (9–10), 512–533.

Debnath, J., Gammoh, N., Ryan, K.M., 2023. Autophagy and autophagy-related pathways in cancer. Nat. Rev. Mol. Cell Biol. 24 (8), 560–575. https://doi.org/10.1038/s41580-023-00585-z.

Dikic, I., Elazar, Z., 2018. Mechanism and medical implications of mammalian autophagy. Nat. Rev. Mol. Cell Biol. 19 (6), 349–364. https://doi.org/10.1038/s41580-018-0003-4.

Erices, J.I., Bizama, C., Niechi, I., Uribe, D., Rosales, A., Fabres, K., Navarro-Martínez, G., Torres, Á., San Martín, R., Roa, J.C., Quezada-Monrás, C., 2023. Glioblastoma microenvironment and invasiveness: new insights and therapeutic targets. Int. J. Mol. Sci. 24 (8), 7047. https://doi.org/10.3390/ijms24087047.

Fernandes, C., Costa, A., Osório, L., Lago, R.C., Linhares, P., Carvalho, B., Caeiro, C., 2017. Current standards of care in glioblastoma therapy. In: De Vleeschouwer, S. (Ed.), Glioblastoma [internet]. Codon Publications, Brisbane (AU). Chapter 11.

Fitzwalter, B.E., Towers, C.G., Sullivan, K.D., et al., 2018. Autophagy inhibition mediates apoptosis sensitization in cancer therapy by relieving FOXO3a turnover. Dev. Cell. https://doi.org/10.1016/j.devcel.2018.02.014.

Foglio, E., Puddighinu, G., Germani, A., et al., 2017. HMGB1 Inhibits apoptosis following mi and induces autophagy via mTORC1 inhibition. J. Cell. Physiol. https://doi.org/10.1002/jcp.25576.

Freitas, L.B., Borgati, T.F., de Freitas, R.P., et al., 2014. Synthesis and antiproliferative activity of 8-hydroxyquinoline derivatives containing a 1,2,3-triazole moiety. Eur. J. Med. Chem. 84, 595–604. https://doi.org/10.1016/j.ejmech.2014.07.061.

GBD 2016 Brain and Other CNS Cancer Collaborators, 2019. Global, regional, and national burden of brain and other CNS cancer, 1990–2016: a systematic analysis for the Global Burden of Disease Study 2016. Lancet Neurol. 18 (4), 376–393. https://doi.org/10.1016/S1474-4422(18)30468-X.

Jain, S., Chandra, V., Kumar, P., Pathak, K., Pathak, D., Vaidya, A., 2016. Comprehensive review on current developments of quinoline-based anticancer agents. Arab. J. Chem. https://doi.org/10.1016/j.arabjc.2016.10.009.

Jamsheena, V., Shilpa, G., Saranya, J., Harry, N.A., Lankalapalli, R.S., Priya, S., 2016. Anticancer activity of synthetic bis(indolyl)methane-ortho-biaryls against human cervical cancer (HeLa) cells. Chem. Biol. Interact. 247, 11–21. https://doi.org/10.1016/j.cbi.2016.01.017.

Jia, J.L., Alshamsan, B., Ng, T.L., 2023. Temozolomide chronotherapy in glioma: a systematic review. Curr. Oncol. 30 (2), 1893–1902. https://doi.org/10.3390/curroncol30020147.

Kannaiyan, R., Mahadevan, D., 2018. A comprehensive review of protein kinase inhibitors for cancer therapy. Expert Rev. Anticancer Ther. https://doi.org/10.1080/14737140.2018.1527688.

Klionsky, D.J., et al., 2021. Autophagy in major human diseases. EMBO J. 40, e108863 https://doi.org/10.15252/embj.2021108863.

Klionsky, D.J., Abdelmohsen, K., Abe, A., et al., 2016. Abedin MJ, Guidelines for the use and interpretation of assays for monitoring autophagy. Autophagy 12 (1), 1–222. https://doi.org/10.1080/15548627.2015.1100356.

Klionsky, D.J., Emr, S.D., 2000. Autophagy as a regulated pathway of cellular degradation. Science 290 (5497), 1717–1721. https://doi.org/10.1126/science.290.5497.1717.

Lang, F., Cohen, P., 2001. Regulation and physiological roles of serum- and glucocorticoid-induced protein kinase isoforms. Sci. STKE 108, re17. https://doi.org/10.1126/stke.2001.108.re17.

Lee, H.S., Park, B.S., Kang, H.M., Kim, J.H., Shin, S.H., Kim, I.R., 2021. Role of luteolin-induced apoptosis and autophagy in human glioblastoma cell lines. Medicina (Kaunas) 57 (9), 879. https://doi.org/10.3390/medicina57090879.

Lehrer, S., Rheinstein, P.H., Rosenzweig, K.E., 2018. Glioblastoma multiforme: fewer tumor copy number segments of the SGK1 gene are associated with poorer survival. Cancer Genom. Proteom. 15 (4), 273–278. https://doi.org/10.21873/cgp.20085.

Li, F.S., Weng, J.K., 2017. Demystifying traditional herbal medicine with modern approach. Nat. Plants 3, 17109. https://doi.org/10.1038/nplants.2017.109.

Liang, X., Lan, C., Jiao, G., Fu, W., et al., 2017. Therapeutic inhibition of SGK1 suppresses colorectal cancer. Exp. Mol. Med. 49 (11), e399.

Liu, J., Liu, Y., Wang, Y., Li, C., Xie, Y., Klionsky, D.J., Kang, R., Tang, D., 2023. TMEM164 is a new determinant of autophagy-dependent ferroptosis. Autophagy 19 (3), 945–956. https://doi.org/10.1080/15548627.2022.2111635.

Liu, Y., Zhao, C., Ma, Q., Li, Y., 2019. Sinomenine retards LPS-elicited inflammation via down-regulating CCAT1 in HaCaT cells. Life Sci. 233, 116703 https://doi.org/10.1016/j.lfs.2019.116703.

Matschke, J., Wiebeck, E., Hurst, S., Rudner, J., Jendrossek, V., 2016. Role of SGK1 for fatty acid uptake, cell survival and radioresistance of NCI-H460 lung cancer cells exposed to acute or chronic cycling severe hypoxia. Radiat. Oncol. 11, 75. https://doi.org/10.1186/s13014-016-0647-1.

Onishi, S., Yamasaki, F., Amatya, V.J., Takayasu, T., Yonezawa, U., Taguchi, A., Ohba, S., Takeshima, Y., Horie, N., Sugiyama, K., 2022. Characteristics and therapeutic strategies of radiation-induced glioma: case series and comprehensive literature review. J. Neuro-Oncol. 159, 531–538. https://doi.org/10.1007/s11060-022-04090-9.

Ortuso, F., Amato, R., Artese, A., D'antona, L., et al., 2014. In silico identification and biological evaluation of novel selective serum/glucocorticoid-inducible kinase 1 inhibitors based on the pyrazolo-pyrimidine scaffold. J. Chem. Inf. Model. 54, 1828–1832. https://doi.org/10.1021/ci500235f.

Sang, Y., Kong, P., Zhang, S., Zhang, L., et al., 2021. SGK1 in human cancer: emerging roles and mechanisms. Front. Oncol. 10, 608722 https://doi.org/10.3389/fonc.2020.608722.

Schmidt, E.M., Gu, S., Anagnostopoulou, V., Alevizopoulos, K., Föller, M., Lang, F., Stournaras, C., 2012. Serum- and glucocorticoid-dependent kinase-1-induced cell migration is dependent on vinculin and regulated by the membrane androgen receptor. FEBS J. 279 (7), 1231–1242. https://doi.org/10.1111/j.1742-4658.2012.08515.x.

Sherk, A.B., Frigo, D.E., Schnackenberg, C.G., et al., 2008. Development of a small-molecule serum- and glucocorticoid-regulated kinase-1 antagonist and its evaluation as a prostate cancer therapeutic. Cancer Res. 68 (18), 7475–7483. https://doi.org/10.1158/0008-5472.CAN-08-1047.

Tan, A.C., Ashley, D.M., López, G.Y., Malinzak, M., Friedman, H.S., Khasraw, M., 2020. Management of glioblastoma: state of the art and future directions. CA Cancer J. Clin. 70 (4), 299–312. https://doi.org/10.3322/caac.21613.

Tian, S., Wang, X., Proud, C.G., 2017. Oncogenic MNK signalling regulates the metastasis suppressor NDRG1. Oncotarget 8 (28), 46121–46135. https://doi.org/10.18632/oncotarget.17555.

Wan, S., Zhang, G., Liu, R., Abbas, M.N., Cui, H., 2023. Pyroptosis, ferroptosis, and autophagy crosstalk in glioblastoma opens up new avenues for glioblastoma treatment. Cell Commun. Signal 21 (1), 115. https://doi.org/10.1186/s12964-023-01108-1.

Xiang, X., Tian, Y., Hu, J., Xiong, R., Bautista, M., Deng, L., Yue, Q., Li, Y., Kuang, W., Li, J., Liu, K., Yu, C., Feng, G., 2021. Fangchinoline exerts anticancer effects on colorectal cancer by inducing autophagy via regulation AMPK/mTOR/ULK1 pathway. Biochem. Pharmacol. 186, 114475 https://doi.org/10.1016/j.bcp.2021.114475.

Zhang, T., Zhou, C., Lv, M., Yu, J., et al., 2024. Trifluoromethyl quinoline derivative targets inhibiting HDAC1 for promoting the acetylation of histone in cervical cancer cells. Eur. J. Pharm. Sci. 194, 106706 https://doi.org/10.1016/j.ejps.2024.106706.

Zheng, X., Li, W., Xu, H., Liu, J., Ren, L., Yang, Y., Li, S., Wang, J., Ji, T., Du, G., 2021. Sinomenine ester derivative inhibits glioblastoma by inducing mitochondria-dependent apoptosis and autophagy by PI3K/AKT/mTOR and AMPK/mTOR pathway. Acta Pharm. Sin. B 11 (11), 3465–3480. https://doi.org/10.1016/j.apsb.2021.05.027.